Supplemental Material for "Rapid optimal work extraction from a quantum-dot information engine"

Kushagra Aggarwal,[1,*] Alberto Rolandi,[2,3,*] Yikai Yang,[1] Joseph Hickie,[4] Daniel Jirovec,[5] Andrea Ballabio,[6] Daniel Chrastina,[6] Giovanni Isella,[6] Mark T. Mitchison,[7,8] Martí Perarnau-Llobet,[9,10,†] and Natalia Ares[1,‡]

[1] *Department of Engineering Science, University of Oxford, Parks Road, Oxford OX1 3PJ, United Kingdom*
[2] *Département de Physique Appliquée, Université de Genève, 1211 Genève, Switzerland*
[3] *Atominstitut, TU Wien, 1020 Vienna, Austria*
[4] *Department of Materials, University of Oxford, Parks Road, Oxford OX1 3PH, United Kingdom*
[5] *Institute of Science and Technology Austria, Am Campus 1, 3400 Klosterneuburg, Austria*
[6] *L-NESS, Physics Department, Politecnico di Milano, via Anzani 42, 22100, Como, Italy*
[7] *School of Physics, Trinity College Dublin, College Green, Dublin 2, D02 K8N4, Ireland*
[8] *Trinity Quantum Alliance, Unit 16, Trinity Technology and Enterprise Centre, Pearse Street, Dublin 2, D02 YN67, Ireland*
[9] *Física Teòrica: Informació i Fenòmens Quàntics, Department de Física, Universitat Autònoma de Barcelona, 08193 Bellaterra (Barcelona), Spain*
[10] *Département de Physique Appliquée, Université de Genève, 1211 Genève, Switzerland*

A. DEVICE FABRICATION

The devices were processed in the Institute of Science and Technology Austria Nanofabrication facility. A 6x6 mm^2 chip comprising of Ge quantum well sandwiched between $Si_{0.3}Ge_{0.7}$ is cleaned before further processing. Further details about the quantum well growth can be found in Ref. [1]. First, ohmic contacts are patterned in a 100 keV electron beam lithography system. Subsequently, a few nanometers of native oxide is milled by argon bombardment which is followed by deposition of 60 nm Pt layer. A 20 nm thick layer of aluminium oxide is deposited at 300°C in an atomic layer deposition step, followed by gates consisting of 3 nm Ti and 27 nm Pd.

B. CHARACTERISATION OF THE TUNNEL RATES AND LEVER ARM

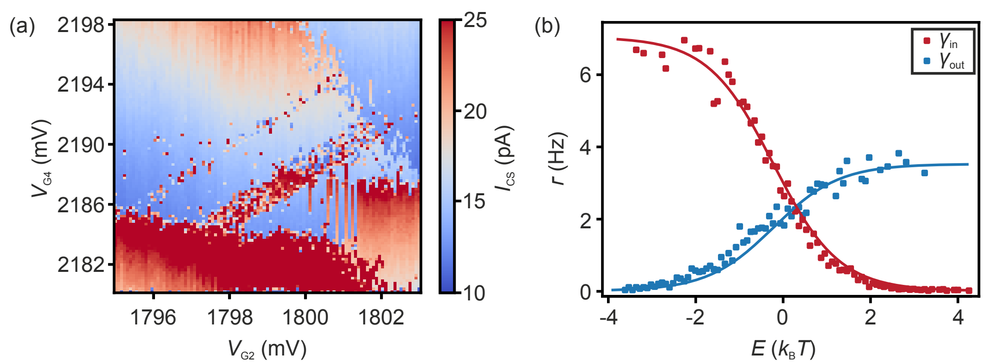

FIG. B1. (a) A set of bias triangles measured by varying V_{G2} and V_{G4} and recording the current I_{CS} through the charge sensor at a bias voltage $V_{b,QD} = 0.32$ mV. (b) Tunneling rates γ_{in} and γ_{out} of QD1.

The measurements were performed in a dilution refrigerator at a base temperature of 150 mK. The charge sensor and the double quantum dot are isolated by creating an electrostatic barrier using splitter gate voltages $V_{S1\text{-}S2}$. The double quantum dot in the bottom array is tuned by using the gates voltages V_{G2} and V_{G4}. The tunneling between Fermi reservoirs and double quantum dot is controlled using gate voltages V_{G1} and V_{G5}. The inter-dot tunneling is set by the gate voltage V_{G3}. Similarly, the charge sensor is tuned by a combination of gate voltages $V_{CS1\text{-}CS3}$. We

* These authors have contributed equally to this work.
† marti.perarnau@uab.cat
‡ natalia.ares@eng.ox.ac.uk

first measure a set of bias triangles, as shown in Fig. **B1(a)**, at a fixed bias $V_{\mathrm{b,\,QD}} = 0.32$ mV. We extract a lever arm $\alpha = \frac{V_{\mathrm{b,QD}}}{\Delta V_{\mathrm{G2}}} = 0.041 \pm 0.002$. Time traces across the transition from $n = 0$ to $n = 1$ were recorded. Tunnel rates and electron temperature were extracted in Fig. **B1(b)** using the functions: $\gamma_{\mathrm{in}} = \Gamma_{\mathrm{in}} f(E)$ and $\gamma_{\mathrm{out}} = \Gamma_{\mathrm{out}}(1 - f(E))$, where $f(E) = (1 + e^{E/k_{\mathrm{B}}T})^{-1}$, which describe the tunneling in and out rates of the quantum dot [2]. We obtain an electron temperature of $T = 180$ mK from these fits.

C. CALIBRATION DRIFT

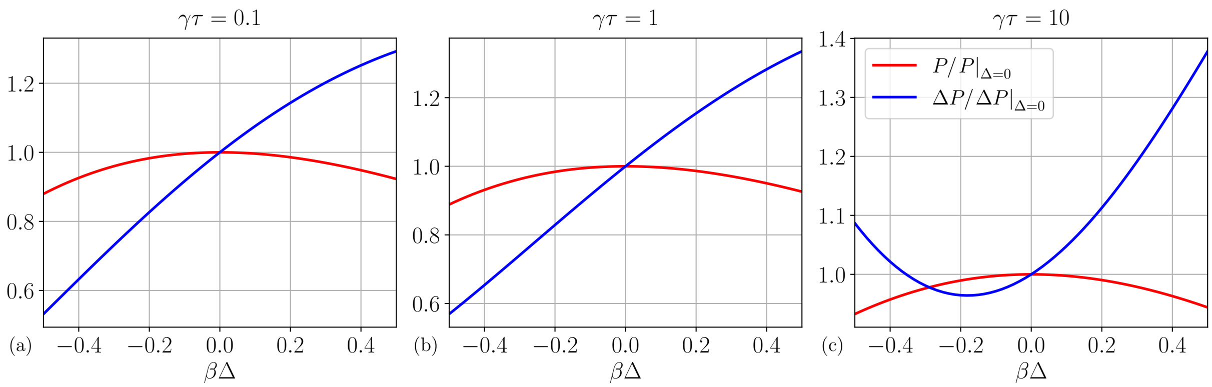

FIG. C2. Relative change of power and fluctuations for a constant shift from the optimal protocol $\varepsilon(t) \to \varepsilon(t) + \Delta$ for all the regimes of driving speeds: (a) $\gamma\tau = 0.1$, (b) $\gamma\tau = 1$, (c) $\gamma\tau = 10$.

Since the calibration drift takes much longer than the duration of a single cycle (even in the slow driving regime) we can assume that within a cycle it corresponds to a constant shift of the energy $\varepsilon \to \varepsilon + \Delta$. In Fig. **C2** we show how this shift affects the power and fluctuations relative to their value in absence of the shift. As expected, since the power is optimal for $\Delta = 0$, we see that for small shifts it deviates from its optimal value as $\mathcal{O}(\Delta^2)$. Conversely, it is clear that this is not the case for ΔP since the protocols do not optimise the fluctuations. Therefore its deviations scale as $\mathcal{O}(\Delta)$. This makes the fluctuations more sensitive than the power to this shift caused by the calibration drift.

D. MEASUREMENT STATISTICS

In this section we present how to compute the estimators – and their variance – for expected work and work fluctuations that were used for the plotted values and error bars in Fig. **2**. For N i.i.d statistical samples $\{W_i\}_{i=1}^N$ of a random variable $\mathcal{W}$. We estimate the expected value of $\mathcal{W}$ with the mean:

$$E(\{W_i\}_{i=1}^N) := \frac{1}{N}\sum_{i=1}^{N} W_i \ . \tag{D1}$$

It is straightforward to compute the expected value and variance of this estimator:

$$\langle E(\{W_i\}_{i=1}^N)\rangle = \langle \mathcal{W}\rangle \ , \tag{D2}$$

$$\mathrm{Var}(E(\{W_i\}_{i=1}^N)) = \frac{\mathrm{Var}(\mathcal{W})}{N} \ . \tag{D3}$$

Therefore, with N samples of work gain $\{W_i\}_{i=1}^N$, we compute the expected work with the estimator E and use the square root of its variance for its error in the plots. To compute the variance from the sample, we use the following estimator

$$V(\{W_i\}_{i=1}^N) = \frac{1}{N-1}\sum_{i=1}^{N}\left(W_i - E(\{W_i\}_{i=1}^N)\right)^2 \ , \tag{D4}$$

which we can use also to estimate the fluctuations of the work gain. The expected value and variance of this estimator give

$$\langle V(\{W_i\}_{i=1}^N)\rangle = \mathrm{Var}(\mathcal{W}) \ , \tag{D5}$$

$$\mathrm{Var}(V(\{W_i\}_{i=1}^N)) = \langle \mathcal{W}^4\rangle \frac{N(N-4)+1}{N(N-1)^2} - \frac{4\langle\mathcal{W}^3\rangle\langle\mathcal{W}\rangle}{N} - \frac{\mathrm{Var}(\mathcal{W})^2}{N-1} + \frac{3\langle\mathcal{W}^2\rangle^2}{N} \ , \tag{D6}$$

where we can use the maximum likelihood estimators for the 2nd, 3rd and 4th moments – m_2, m_3 and m_4 respectively – to compute the error of the estimator of the work fluctuations from the statistical samples. These maximum likelihood estimators are given by

$$m_j(\{W_i\}_{i=1}^N) := \frac{1}{N}\sum_i W_i^j \ , \tag{D7}$$

and satisfy $\langle m_j(\{W_i\}_{i=1}^N)\rangle = \langle \mathcal{W}^j\rangle$.

[1] D. Jirovec, A. Hofmann, A. Ballabio, P. M. Mutter, G. Tavani, M. Botifoll, A. Crippa, J. Kukucka, O. Sagi, F. Martins, J. Saez-Mollejo, I. Prieto, M. Borovkov, J. Arbiol, D. Chrastina, G. Isella, and G. Katsaros, Nature Materials **20**, 1106–1112 (2021).

[2] A. Hofmann, V. F. Maisi, C. Rössler, J. Basset, T. Krähenmann, P. Märki, T. Ihn, K. Ensslin, C. Reichl, and W. Wegscheider, Phys. Rev. B **93**, 035425 (2016).